Reactive crystal growth in two dimensions: Silicon nitride on Si(111)

E. Bauer,* Y. Wei, T. Müller,* A. Pavlovska,* and I. S. T. Tsong
Department of Physics and Astronomy, Arizona State University, Tempe, Arizona 85287-1504
(Received 9 January 1995)

The nitridation of the Si(111) surface by reaction with NH_3 was studied by low-energy electron microscopy (LEEM), low-energy electron diffraction (LEED), and scanning tunneling microscopy (STM). Reaction layers with periodicities of (8×8), $(\frac{8}{3}\times\frac{8}{3})$, $(\frac{3}{4}\times\frac{3}{4})$, and $(3\sqrt{3}/4\times3\sqrt{3}/4)$ were observed depending on the temperature of nitridation and duration of electron-beam exposure. The nucleation and growth of the nitride layer on well-oriented and miscut Si(111) surfaces were observed by STM and followed in real time by video LEEM. The (8×8) nitride islands nucleate and grow in the same manner as the (7×7) domains, with the apex of the triangle pointing in the $[\bar{1}\,\bar{1}2]$ direction away from the step into the upper terrace. On the miscut surface, (8×8) nitride growth proceeds with widening of the terraces and step bunching. The $(\frac{3}{4}\times\frac{3}{4})$ multiplet structure, on the other hand, nucleates randomly on comtaminated sites on the surface, or evolves directly from the (8×8) structure.

I. INTRODUCTION

The past decade has seen numerous studies of the growth of metals and semiconductors on single-crystal surfaces by various imaging techniques such as scanning tunneling microscopy (STM), low-energy electron microscopy (LEEM), reflection electron microscopy, and scanning electron microscopy. These studies have advanced our understanding of nonreactive deposition and growth to a considerable extent. By contrast, very few microscopic studies have been undertaken on reactive deposition and growth, silicide formation being perhaps the only exception. Accordingly, the goal of our present work is to achieve a better understanding of the processes that occur during thin-film growth caused by gas-surface reactions. As a model system, we have chosen the growth of a nitride layer during the reaction of NH_3 with Si(111). Silicon nitride layers on silicon have attracted considerable interest for some time, mainly because of their practical importance in microelectronics.[1,2] In these applications they are usually deposited by chemical-vapor deposition from a mixture of silicon-hydrogen and nitrogen-hydrogen compounds such as SiH_4, Si_2H_6, Si_3H_8, NH_3, N_2H_4, and HN_3.[3] The resulting a-SiN_x:H layers are generally amorphous, nonstoichiometric, and contain hydrogen. Nitride layers can, however, also be grown without Si supply from the gas phase by direct nitridation. The (111) face, with which this paper is concerned, has been nitrided in this manner with nitrogen atoms,[4–6] ions,[7,8] NH_3,[8–18] NO,[12,13,19–22] and other gaseous N compounds,[23,24] either directly at high temperatures or by annealing at high temperatures after low-temperature exposure.

A wide range of laterally averaging surface probes has been used to study the growth and structure of thermal nitride layers, such as low-energy electron diffraction (LEED),[4,6–11,17,21,24] reflection high-energy electron diffraction,[8,10] electron-energy-loss fine-structure measurements,[6] Auger-electron spectroscopy (AES),[4,6,7,11,16–21,24] electron-energy-loss spectroscopy (EELS),[4,12,17] x-ray photoelectron spectroscopy,[8,15,19,23,24] ultraviolet photoelectron spectroscopy,[13,15,19,22–24] photoemission yield spectroscopy,[17] high-resolution (vibrational) electron-energy-loss spectroscopy (HREELS),[5,14,20,21,23,24] thermal-desorption spectroscopy (TDS),[4,16,19] and laser-induced thermal desorption.[16] These studies have produced a wealth of partially contradicting information, to be summarized shortly, on the laterally averaged features of the layers. Little is known, however, about the kinetics of the nitridation process or about the atomic and microstructure of the resulting layer. The aim of this paper is to fill this gap by combining LEEM/LEED and STM in a study of the high-temperature nitridation of Si(111) by NH_3. The (111) surface is of particular interest because contrary to the (100) surface which retains a $p(2\times1)$ structure after high-temperature nitridation,[25] two ordered nitride structures have been reported for the (111) surface as described below.

From the laterally averaging studies, the following general picture emerges. Upon N atom or ion bombardment, the first signs of order in the overlayer appear at 700 K, but good long-range order with a (8×8) periodicity is not achieved until about 1000 K. Nitridation with nitrogen-containing molecules requires desorption of the coadsorbate before an ordered nitride layer can form, e.g., about 1000 K for NH_3, N_2H_4, or HN_3, and about 1150 K for NO. Once only N is present on the surface, a well-ordered (8×8) LEED pattern is observed up to about 1150 K. Between approximately 1150 and 1250 K, this pattern coexists with another one, originally named doublet or quadruplet pattern, but in this paper it will be called a multiplet pattern (MP). Above 1250 K, only the MP is observed until the desorption of the nitride in the form of Si_2N molecules is completed at approximately 1400 K.[4] The temperatures vary considerably from author to author, partly because of the different structural information of the various techniques, and partly because

of the difficulties of exact temperature measurements on Si. Much larger discrepancies exist between the coverages and thicknesses ascribed to nitride layers in various growth stages. For example, the (8×8) pattern were attributed to a N coverage of 1.89 Si ML (Ref. 4) or 15-Å nitride thickness,[8] and the MP to a coverage of 3.55 Si ML (2 atoms/MP unit cell)[4] or a thickness of 15 Å.[8] The early stages of growth of both structures were attributed to the formation of a chemically reacted monolayer, which grew in islands.[4] Another study[18] claimed that the initially formed nitride islands were 5±1 Å thick. A limiting thickness of 25–30 Å was deduced from AES measurements,[4] while other authors reported growth—though slow—beyond 40 Å.[8] From TDS measurements,[4] a saturation coverage of 5.5 and 8.5 times the monolayer coverage was estimated for the (8×8) and the MP structures, respectively. The order in the layer decreased rapidly with thickness beyond 1 ML. At the multilayer growth stage, a Frank–van der Merwe (layer-by-layer) growth mode for the MP structure and a Stranski-Krastanov (layer+island) growth mode for the mixed (8×8) and MP structure were suggested.[4]

Only limited information on the atomic structure could be extracted from the laterally averaging studies. The (8×8) and MP structures have been attributed to nitride overlayers with unit-cell dimensions of $\frac{8}{11}$ and $\frac{3}{4}$ of the Si(111)-(1×1) unit-cell dimensions, respectively.[4,10] According to HREELS measurements, the lattice in both cases is a honeycomb mesh with Si and N alternating on its lattice sites, such that each N atom is surrounded by 3 Si atoms in a near-planar and planar configuration in the (8×8) and MP structure, respectively.[20]

Many other details have been deduced from the laterally averaging studies, some of which will be used later in the discussion of the laterally resolving studies reported here. Our studies not only aim at an understanding of the atomic and microstructure of the layer, but also at the understanding of its growth kinetics.

II. EXPERIMENT

The experiments were conducted in two systems: in a commercial LEEM (Ref. 26) and in a home-built STM. Both instruments have a base pressure in the 10^{-11} torr range. In the STM, the Si(111) sample was cleaned by flashing to 1450 K to obtain the (7×7) reconstruction. All STM images were taken at room temperature. The experiments were carried out by dc resistive heating of the Si(111) crystal to the desired temperatures of 1220 and 1320 K (±10 K), and then exposing the hot crystal at 2×10^{-7} torr NH_3 for 10 sec (low coverage) or 6×10^{-7} torr NH_3 for 15 min (high coverage). Some of the layers were also annealed subsequently 50–100 K above the reaction temperature. Two crystals were used, one oriented to $<0.1°$ of the (111) orientation, the other one with an intentional miscut of 2.5° in the $[11\bar{2}]$ direction. The STM studies were undertaken in order to augment the resolution-limited LEEM studies with atomic resolution and the reciprocal-space information from LEED with real-space information.

The bulk of the experiments was carried out in the LEEM, combined with LEED, photoelectron emission microscopy (PEEM), and mirror electron microscopy (MEM). When the nitride layer disordered with increasing thickness, MEM and LEEM at very low energies (≤ 1 eV) were particularly useful. The Si(111) surface was exposed to NH_3 in direct line of sight of the gas doser consisting of a copper tube with a microchannel plate mounted at the front end, which allowed pressure differences of two orders of magnitude between inlet system and the LEEM sample chamber. Due to the directional flow from the NH_3 source, the effective pressure at the sample surface was significantly higher than the chamber pressure measured with the ion gauge. Therefore, some experiments were also conducted using a nondirectional gas inlet or the residual NH_3 pressure, which decreased slowly with time after high exposures. The residual gas consisted mainly of NH_3 with some H_2 and N_2, as determined by a quadrupole mass spectrometer mounted in the sample chamber. Because of the different nitridation procedures, all exposures will be expressed in pressure and time rather than in langmuirs.

Prior to nitridation in the LEEM, the sample holder with an oxidized Si(111) crystal were carefully outgassed below 1000 K. The oxide layer was then removed by flashing the Si(111) sample to increasingly higher temperatures, while simultaneously keeping the pressure below 5×10^{-9} torr until a (7×7) LEED pattern was obtained. For certain nitridation experiments, an intentionally carbon-contaminated surface was required. This was indicated by a grainy surface structure in the LEEM images.[27] In the majority of nitridation experiments, the sample was first heated to the desired temperature and then the NH_3 gas supply was turned on. However, other heating procedures were also used, such as heating the sample first to a temperature higher than the Si_2N desorption temperature before quenching rapidly to the chosen reaction temperature, and reacting at a lower temperature before heating stepwise to increasingly higher temperatures. The temperature of the sample was measured with a thermocouple attached to the sample holder and also directly with an infrared pyrometer. Low- and high-temperature calibration points were the melting point of Pb (600 K) deposited *in situ* on the Si(111) surface and the (7×7)↔(1×1) phase-transition point at 1110 K.[28]

Two types of Si(111) wafers were used in the LEEM; one was well-oriented ($\leq 0.05°$), and the other with the standard orientation of ±0.5°. Because of the frequent switching between different operation modes (LEEM, PEEM, MEM, LEED) no effort was made to correct the distortions of the LEED pattern, but all reciprocal lattice distances measured are nevertheless accurate to better than 1%, due to the use of the (7×7) structure as a correction measure.

III. RESULTS AND DISCUSSION

A. Atomic structure

The information on the atomic structure of the nitride layer obtained in the past was derived mainly from

LEED and HREELS. In the present study, the main difference from the previous LEED studies is the extension of the energy range to lower energies. All previously published LEED patterns[4,6,9–11] were obtained at energies between 35 and 70 eV. In the LEEM instrument, the LEED pattern can be observed down to zero energy. The wide energy range accessible allows a better distinction between single and multiple diffraction. At higher energies, 35–70 eV, multiple scattering between monoatomic overlayer and the substrate is strong because direct elastic backscattering is weak. At low energies, for example at 6.5 eV as shown in Fig. 1(a), double scattering between overlayer and substrate is not possible because the Ewald sphere is too small to excite the substrate (10) reflections. At high energies, the (11,0) spots of the (8×8) pattern are very strong, which has led previous authors to interpret these spots as the (1,0) spots of an overlayer with a lattice constant $a=(8/11)a_{\mathrm{Si}(111)}=2.79$ Å, where $a_{\mathrm{Si}(111)}=3.84$ Å. At low energies in Fig. 1(a), the (3,0) spots are dominating, which leads us to conclude that the overlayer periodicity is $a=(8/3)a_{\mathrm{Si}(111)}=10.24$ Å. Additional weaker spots of the (8×8) pattern indicate a modulation of this "$(\frac{8}{3}\times\frac{8}{3})$" structure with the periodicity of the (8×8) coincidence mesh. A full (8×8) plus sextet LEED pattern taken at a higher energy, 28 eV, is shown in Fig. 1(b).

STM confirms this interpretation. Careful measurements of the STM image of the (8×8) structure in Fig. 2, in particular of its Fourier transform using that of an adjoining (7×7) region as a reference, give a periodicity of $(2.63\pm0.06)a_{\mathrm{Si}(111)}$, which agrees within the limits of error with the more accurate LEED result of $(\frac{8}{3})a_{\mathrm{Si}(111)}\approx 2.67a_{\mathrm{Si}(111)}$. When viewed along the "atomic" rows a weak threefold modulation is visible in Fig. 2, which is in agreement, i.e., 3×8/3, with the eightfold modulation derived from LEED. STM images of the nitride layers could be obtained only at high biases, + or − 3 V and above. This is understandable if the local density of states of the nitride layer is similar to that of bulk Si_3N_4, which has a band gap of about 5 eV.[1] Tunneling occurs most likely to Si atoms with the weakest Si-N interaction. Additional information comes from the step height between a lower (7×7) terrace and an upper (8×8) terrace at low coverage. It is (2.1±0.1) Å, which is only 67% of the Si(111) step height, though significantly larger than the thickness of a monolayer of Si_3N_4 ($d=1.45$ Å) consisting of planar NSi_3 clusters. The value 2.1±0.1 Å agrees well with the monolayer thickness derived from AES,[6] but is incompatible with the (8×8) island thickness reported by other authors.[18] Finally, from previous HREELS data, it was deduced that the (8×8) layer consists of relatively flat N-Si py-

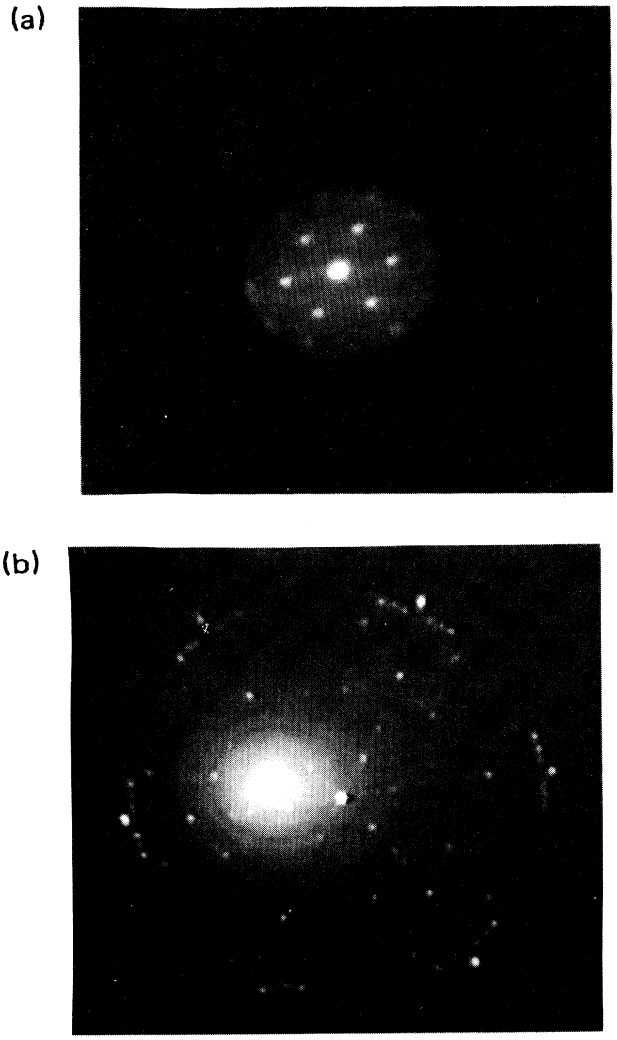

FIG. 1. LEED patterns of layers obtained by nitridation of Si(111) at 1140 K at 1×10^{-7} torr of NH_3 for 15 min: (a) Taken at 6.5 eV. Only the low-order beams of the (8×8) pattern appear. (b) Taken at 28 eV, showing the (8×8) plus sextet pattern. Higher-order beams, in particular the dominating $\frac{11}{8}$ order, are present.

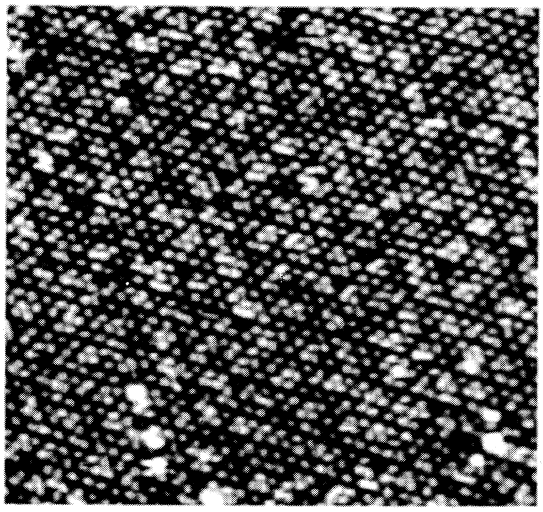

FIG. 2. A 365×365 Å^2 STM image of a nitride layer with $(\frac{8}{3}\times\frac{8}{3})$ structure. Nitridation of the Si(111) surface occurred at 1220 K at 6×10^{-7} torr of NH_3 for 15 min. Sample bias = −4.0 V.

ramids,[5,14,20,21,23,24] though this has been refuted on the basis of EELS measurements.[6]

The relationship between the $\frac{8}{3}$-fold periodicity observed in the present LEED and STM results and the eightfold periodicity is illustrated in real space in Fig. 3(a). The dotted lines outline the $(\frac{8}{3}\times\frac{8}{3})$ unit cell of the overlayer (open circles), while the dashed lines outline the (8×8) unit cell of the coincidence mesh. The black dots indicate the periodicity of Si(1×1) surface without favoring any particular lateral registration. A proposed structure for $(\frac{8}{3}\times\frac{8}{3})$ is shown in Fig. 3(b). The $(\frac{8}{3}\times\frac{8}{3})$ unit cell is chosen to coincide with the Si atom located at the center of a Si-N honeycomb, believed to be the tunneling site, i.e., a bright spot in Fig. 2. Each N atom (shaded circle) is surrounded by three Si atoms (open circles) and the composition of the layer is Si_5N_3. The structure in Fig. 3(b) is idealized. Due to the interaction with the underlying Si substrate, atom displacements to optimize bonding are expected. Our proposed model is compatible with all present and previous experimental evidence, while the previously proposed $(8/11\times8/11)$ structure[5,14,20,21,23,24] is incompatible with our LEED and STM results.

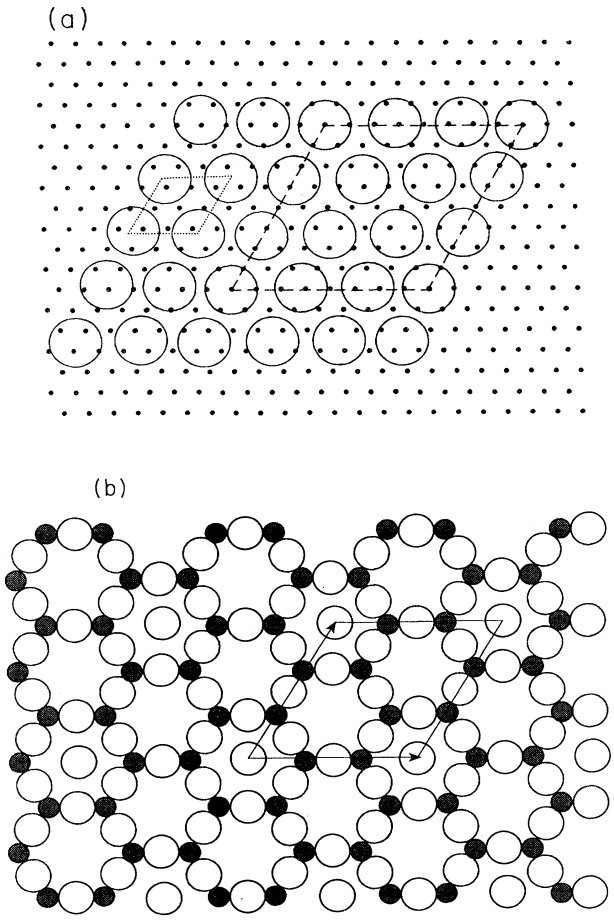

FIG. 3. Structural models showing (a) the relationship between the $(\frac{8}{3}\times\frac{8}{3})$ overlayer and the (8×8) coincidence lattice. The black dots indicate the Si(1×1) positions, while the large open circles represent the bright spots in the STM image. The (8×8) unit cell is outlined by dashed lines and $(\frac{8}{3}\times\frac{8}{3})$ unit cell by dotted lines. (b) The $(\frac{8}{3}\times\frac{8}{3})$ overlayer with the unit cell outlined. The open circles represent Si and shaded circles N.

We now turn to the multiplet pattern, MP. At temperatures ≥ 1140 K, we have observed in LEED several versions of MP: doublet, quadruplet, sextet, and even octet, all appearing in the same nitride layer. Figure 1(b) shows a sextet pattern. In previous work,[4,5,20,21] the LEED pattern for the MP was attributed to a planar hexagonal lattice with a periodicity of $a\approx(\frac{3}{4})a_{\mathrm{Si}(111)}$. The $(\frac{3}{4}\times\frac{3}{4})$ structure consists of domains azimuthally rotated at some small angles, depending on the splitting, with respect to the Si(111) surface. Since we have not observed any strong LEED spots at low energies in the MP, we agree with the previous assignment of the $(\frac{3}{4}\times\frac{3}{4})$ structure, a model of which is shown in Fig. 4(a). However, in re-

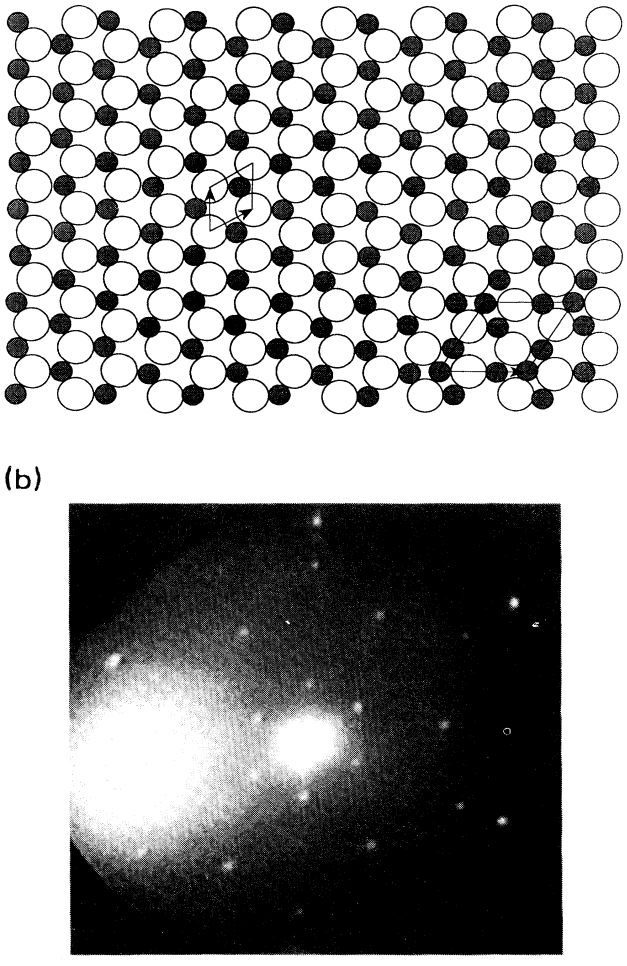

FIG. 4. (a) A model of the $(\frac{3}{4}\times\frac{3}{4})$ multiplet structure showing planar SiN honeycombs. The $(\frac{3}{4}\times\frac{3}{4})$ unit cell is shown near the center. The open circles represent Si and the shaded circles N. A $(3\sqrt{3}/4\times3\sqrt{3}/4)$ unit cell is shown in the corner by adding extra N atoms in the center of the honeycombs to represent the singlet structure. (b) A singlet LEED pattern showing the extra $(3\sqrt{3}/4\times3\sqrt{3}/4)$ spots. Taken at electron energy 33.6 eV.

gions of the nitride layer subjected to prolonged electron irradiation, we found that the MP degenerated into a singlet and the LEED pattern of the $(\frac{3}{4}\times\frac{3}{4})$ structure showed additional $(3\sqrt{3}/4\times3\sqrt{3}/4)$ spots as shown in Fig. 4(b). The singlet pattern implies that the $(\frac{3}{4}\times\frac{3}{4})$ structure is now unrotated with respect to the Si(111) substrate, in contrast to the MP. To account for the $(3\sqrt{3}/4\times3\sqrt{3}/4)$ LEED pattern, we have added extra N atoms in the center of the SiN honeycombs, as shown in the corner of Fig. 4(a). N atoms, rather than Si atoms, appear to be suitable candidates since there are now 3 Si atoms and 4 N atoms in the $(3\sqrt{3}/4\times3\sqrt{3}/4)$ unit cell, resulting in a Si_3N_4 composition. This is likely because the Si_3N_4 layer can be grown to a thickness such that double scattering with the substrate is no longer recognizable. The extra atoms must be bound very strongly because the $(3\sqrt{3}/4\times3\sqrt{3}/4)$ pattern persists until desorption.

Interestingly, we could not resolve any $(\frac{3}{4}\times\frac{3}{4})$ or $(3\sqrt{3}/4\times3\sqrt{3}/4)$ structure in the STM. After nitridation at 1200 K at 6×10^{-7} torr NH_3 for 15 min and annealing at 1300 K, we only encountered structureless three-dimensional islands with flat tops, with widths ranging from 1500 to 4500 Å and heights 3–9 Å, giving an aspect ratio of ~0.002. In the LEEM, where a much larger nitridation parameter range was studied, a wider range of MP particle sizes was found, as will be discussed in the next section.

B. Nucleation and growth

Room-temperature adsorption followed by annealing allows us to make a connection between low-temperature NH_3 adsorption experiments and nitride growth. Previous low-temperature work[14–17] has shown that NH_3 is dissociated at 300 K into NH_2 and H. Saturation is assumed to occur when these two species occupy all 19 dangling bonds in the (7×7) unit cell, which yields a N coverage of $\frac{1}{2}\times\frac{19}{49}\approx0.20$ ML.[17] All previous work shows that nitrogen is not desorbed upon annealing to the (8×8) formation temperature, i.e., 1000–1050 K. Therefore, all N must be incorporated into islands with the (8×8) structure and the N coverage in this structure can be estimated by measuring the areal fraction covered by these islands. At temperatures below 1100 K, the (8×8) islands are so small that the video LEEM images are not suitable for printing. We therefore show in Fig. 5(a) the LEEM image taken with a $\frac{3}{8}$ order beam at 1210 K. The (8×8) crystals not only decorate the Si surface steps, but also the (7×7) domain boundaries similar to other strongly interacting adsorbates, such as the (5×1) structure of Au.[29] The (8×8) coverage deduced from Fig. 5 is 25%. The room-temperature saturation coverage of 0.20 ML is, therefore, concentrated into 0.25 ML, which yields a N coverage in the (8×8) structure of 0.8 ML, in good agreement with the N coverage of 0.844 derived for the (8×8) surface from the model shown in Fig. 3(b).

A nitride growth sequence at 1260 K is shown in Fig. 6. By comparison with the LEEM images of the $(7\times7)\leftrightarrow(1\times1)$ transition in the same region, located by the scratch on the surface in Fig. 6, we deduce that the (8×8) islands nucleate and grow in the same manner as

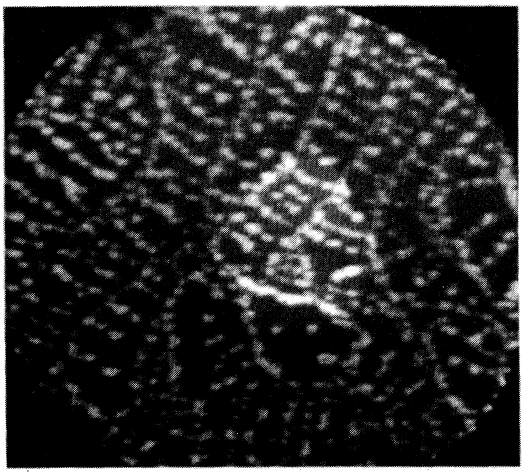

FIG. 5. LEEM image of the Si(111) surface saturated by exposure to 6×10^{-7} torr NH_3 for 15 min at room temperature and then annealed to 1210 K. Taken with $\frac{3}{8}$ order beam. Electron energy 2.7 eV. Field of view 6 μm.

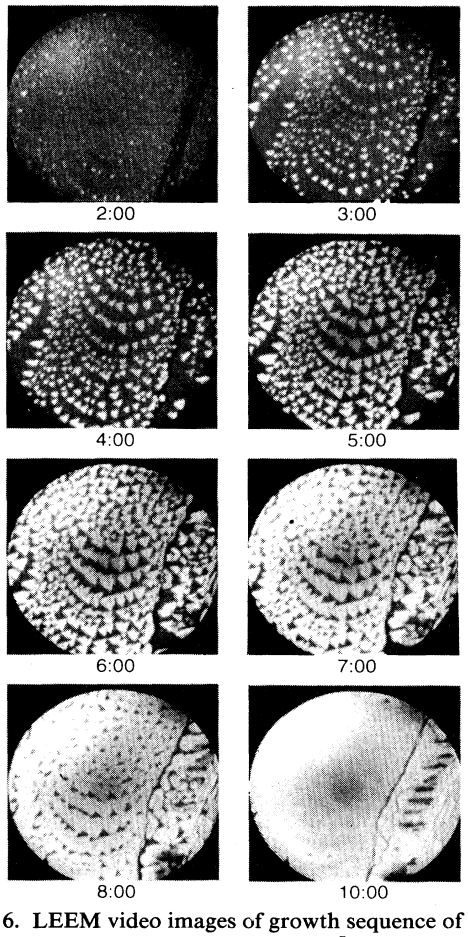

FIG. 6. LEEM video images of growth sequence of (8×8) nitride islands, during exposure to 2×10^{-7} torr NH_3 at 1260 K. Elapsed time in minutes is indicated below each frame, with 0:00 being the time when NH_3 was admitted into the LEEM sample chamber. The (8×8) areas are bright and (1×1) areas dark. The line running north-south on the right-hand side of the images is a scratch on the surface. Electron energy 42 eV. Field of view 10 μm.

the (7×7) domains, i.e., with the apex of the triangle pointing in the $[\bar{1}\,\bar{1}2]$ direction, away from the step into the upper terrace.[28] This indicates that the one-dimensional (8×8)-(1×1) interface is strongly anisotropic with energy minima in the $\langle\bar{1}10\rangle$ directions similar to the (7×7)-(1×1) interface. Despite the similarity, one must bear in mind that the formation of the (7×7) structure is mechanically driven by surface stress caused by the termination of the bulk lattice, resulting in a high density of surface dangling bonds. Whereas the formation of the (8×8) nitride structure is chemically driven, i.e., by the Si-N reaction. In the former case, only Si adatom or interstitial diffusion is sufficient; while in the latter, Si, N, and/or possibly Si_2N molecules are involved.

More detailed information about the nucleation sites comes from low-coverage STM images. Figure 7(a) is representative of the initial nucleation stage. The higher-magnification filled-state image of Fig. 7(b) of an (8×8) island permits the determination of the direction of its apex by comparison with the faulted and unfaulted (7×7) triangles. The result is in complete agreement with the conclusions drawn from LEEM images as described above. The islands are found preferentially, though not exclusively, at convex regions of the steps indicating that they are pinning centers for the step motion. These images were taken with a high bias of −3.5 V. Images taken at the normal tunneling bias of 2 V show that many adatoms, except the corner atoms, are "missing" in the (7×7) region, as previously observed

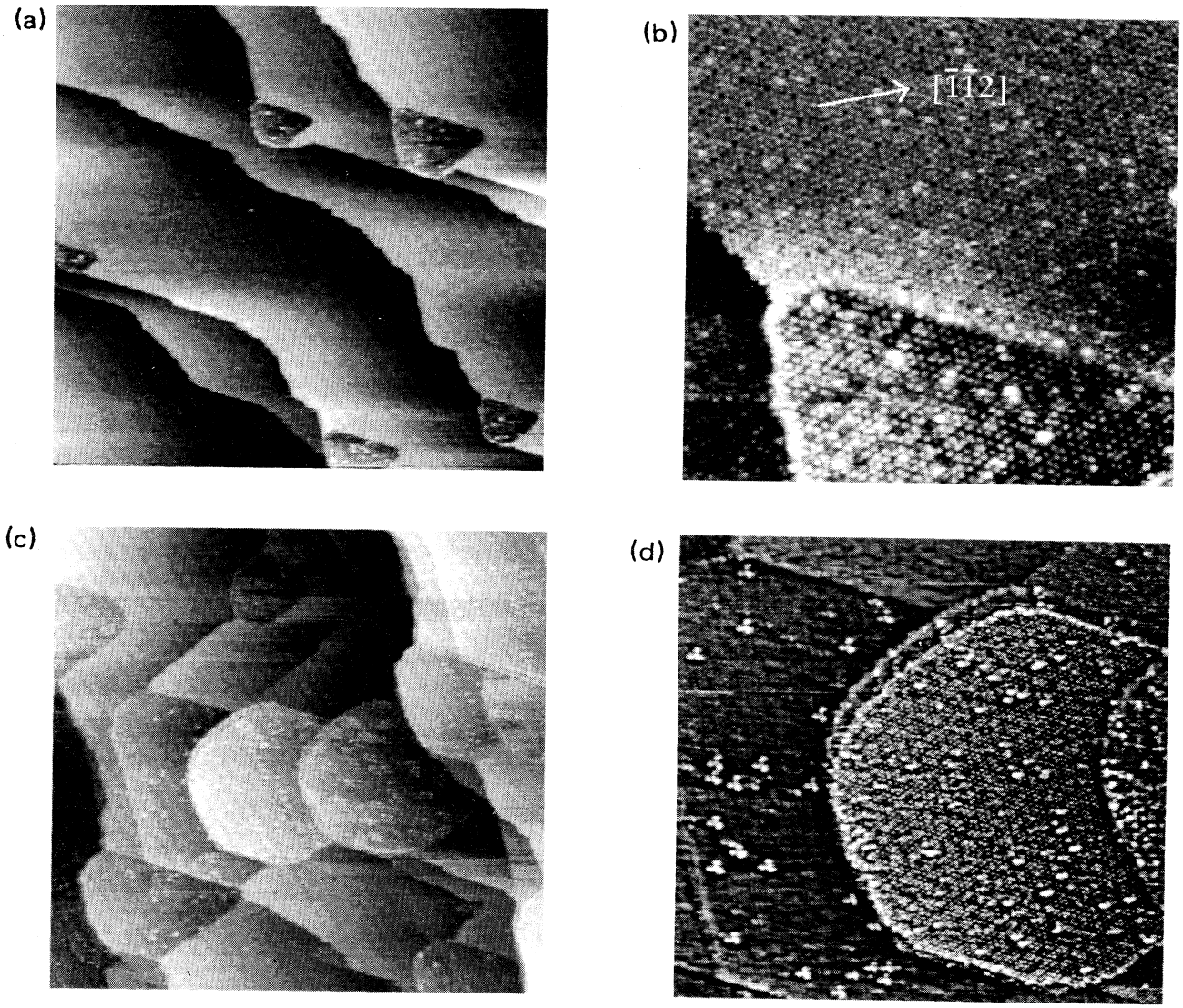

FIG. 7. STM images of initial stages of nitridation. The well-oriented Si(111) surface was exposed to 2×10^{-7} torr NH_3 for 10 sec at 1220 K (a) and (b) and subsequently annealed at 1320 K (c) and (d). Scan areas: (a) 250×250 nm^2, (b) 514×514 $Å^2$, (c) 250×250 nm^2, and (d) 850×850 $Å^2$. Sample bias: (a) and (b) −3.5 V; (c) and (d) 4.0 V. The triangular (8×8) structure is 2.1 Å higher than the lower (7×7) terrace and 1.0 Å below the (7×7) structure on the same terrace in image (b).

during room-temperature adsorption, due to tunneling suppression caused by adsorbed NH_2 and H.[30,31]

Annealing of the surface shown in Figs. 7(a) and 7(b) at 1320 K leads to a considerable change of the (8×8) island morphology as seen in Figs. 7(c) and 7(d). The triangular (8×8) islands transform into a hexagonal shape and the terraces assume a fractured appearance. In the (8×8) regions, many bright triangular triplet clusters are found. The sides of these triangular triplets are approximately oriented along the $[\bar{1}\,\bar{1}2]$ directions. Using the (8×8) structure as a reference, the distance of bright spots in the triplets is about $5a_{Si(111)} = 19.2$ Å. We attribute these features tentatively to small triangular 3D islands with MP structure, which are known to form in this temperature range. The apparent height of these triplet clusters above the (8×8) surface is ~3.1 Å.

Later stages of nitridation of the Si(111) surface are shown in the large-area STM images of Fig. 8. Saturating the surface by an exposure of 15 min at 6×10^{-7} torr NH_3 at 1220 K gives rise to deep holes and large monolayer islands as shown in Fig. 8(a). Annealing this surface at 1320 K produces straight monoatomic glide steps along the $[\bar{1}10]$ direction as shown in Fig. 8(b), due to plastic deformation of the surface caused by the rigid mounting of the sample and rapid cooling. These $[\bar{1}10]$ glide steps have been previously observed in thermally strained Si(111) samples in the LEEM (Ref. 32) and mechanically strained Si(111) samples in the STM.[33] Comparing Fig. 8(a) with 8(b), we can see that subsequent annealing at 1320 K causes breaking up of the terraces into hexagonlike fragments similar to the hexagonal (8×8) islands at low coverage after annealing in Figs. 7(c) and 7(d). Annealing also appears to cause the very bright small features on the terraces in Fig. 8(a) to migrate to the step edges.

In addition to the triangular and hexagonal island shapes, many other morphologies were observed in the LEEM studies. Figure 9 shows a growth sequence obtained at 1180 K after quenching from 1350 K (where no reaction takes place) in 2×10^{-7} torr NH_3. The crystals are dendritic as soon as their shape becomes recognizable. A second layer, as indicated by a different gray level in frame 8:30 of Fig. 8, seems to form before the first layer is completed. In the last frame at 12:30, there are still small gaps between the crystals. The bright particle which grows around a contaminant particle in the two

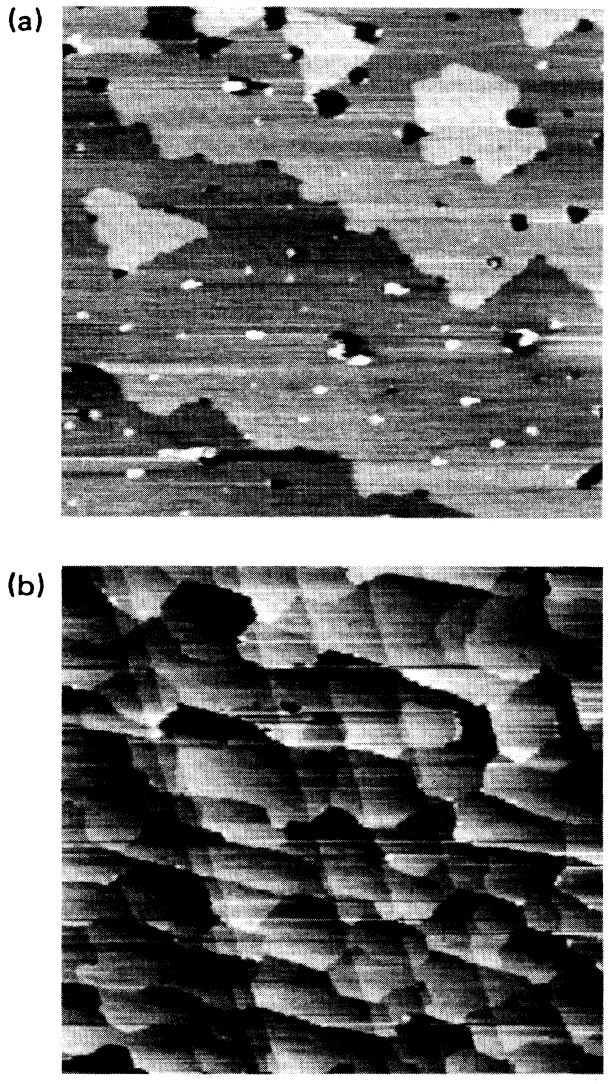

FIG. 8. STM images of a well-oriented Si(111) surface; (a) after exposure to 6×10^{-7} torr NH_3 for 15 min at 1220 K; and (b) subsequently annealed at 1320 K. Scan area is 1×1 μm^2 in both images. Sample bias is 5.0 V.

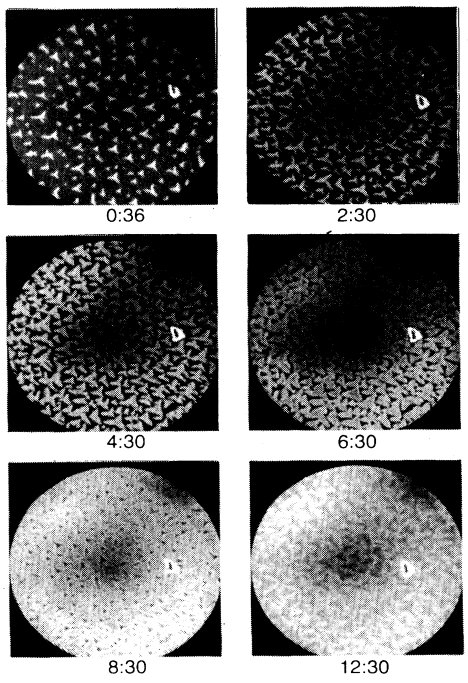

FIG. 9. LEEM video images of growth sequence of dendritic (8×8) nitride islands during exposure to 2×10^{-7} torr NH_3 at 1180 K. Elapsed time in minutes is indicated below each frame. Electron energy 45.4 eV. Field of view 15 μm.

o'clock position has MP structure as identified by its contrast. As we mentioned in the Introduction, (8×8) and MP structures were reported in previous work to coexist between 1150 and 1250 K, and only the MP was observed above 1250 K. We found predominantly (8×8) structure even at 1270 K and had to contaminate the surface intentionally in order to obtain comparable fractions of the two structures. Two growth sequences illustrating this are described below.

In Fig. 10, the crystal was exposed at 1270 K to 1×10^{-7} torr NH_3 after a long series of experiments, which had led to surface contamination as identified by the poor step structure. Repeated subsequent flashing to about 1450 K led to segregation of the impurities into SiC crystals; which appear as small black spots in the first two frames of Fig. 10. These act as pinning centers during the sublimation of Si, which in turn leads to the formation of large flat terraces with few atomic steps separated by step bunches,[27,28] as indicated by denuded (dark) regions in Fig. 10. Although only later growth stages are shown, the bright islands with MP structure appear at the very beginning and do not nucleate on pinning centers. Some MP islands nucleate in the coalescence stage of the (8×8) structure (last frame of Fig. 10) and further MP growth occurs via conversion from the (8×8) structure.

When the surface is heavily contaminated, the MP structure nucleates before the (8×8) structure as shown in Fig. 11. The grainy areas are contaminated by incomplete carbon segregation, while the flat (gray) areas are clean as determined by the (7×7)↔(1×1) phase transition. Many bright MP particles have formed in the contaminated areas before the first (8×8) dendritic-shaped nuclei appear in the clean region in the 2:40 frame. Nucleation and growth of the MP particles occur preferentially at the edge of the contaminated regions, presumably due to the larger supply of N atoms from the flat areas between them. Prolonged exposure beyond that shown in Fig. 11 did not change the relative fractions of the two structures significantly. The influence of contamination for the growth of the MP structure is particularly well demonstrated by Fig. 12, taken from the same experiment as Fig. 10 after long exposure to NH_3 at 1270 K.

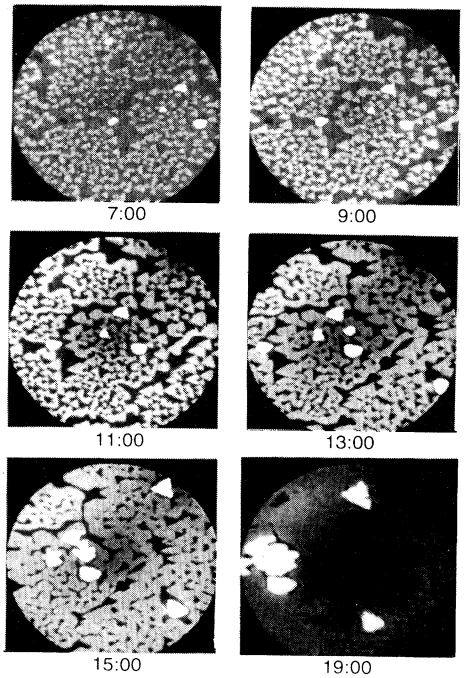

FIG. 10. LEEM images of later growth stages during exposure to 1×10^{-7} torr NH_3 at 1270 K. The brightest areas are $(\frac{3}{4}\times\frac{3}{4})$ multiplet structure islands. Electron energy 42 eV. Field of view 15 μm.

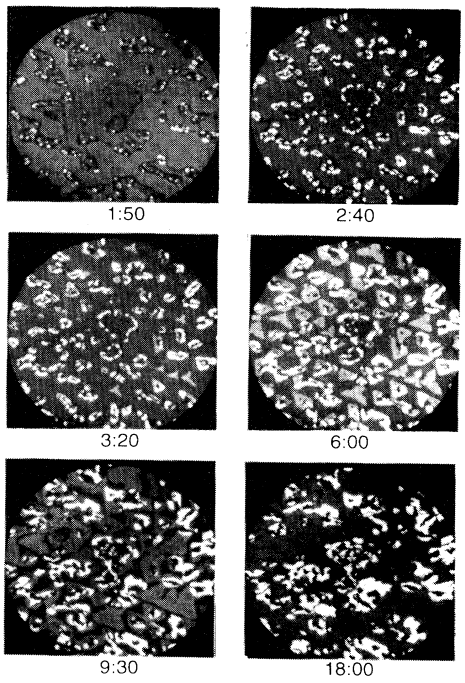

FIG. 11. LEEM growth sequence during exposure to 1.5×10^{-7} torr NH_3 at 1200 K, showing both $(\frac{3}{4}\times\frac{3}{4})$ islands (brightest) and (8×8) islands (less bright). Electron energy 42 eV. Field of view 15 μm.

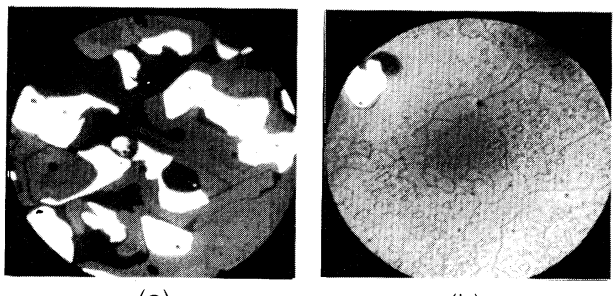

FIG. 12. LEEM images taken in the same growth sequence as in Fig. 10. (a) Area under prolonged electron irradiation after 25:00; and (b) area outside the irradiated region after 30:00. Brightest areas are $(\frac{3}{4}\times\frac{3}{4})$ islands. Electron energy 42 eV. Field of view 15 μm.

The surface region exposed to the electron beam during this experiment is to a considerable extent converted into the MP structure with several azimuthal orientations including the singlet structure, as shown by the bright and dark patches in Fig. 12(a). The surface region outside the electron beam produces an excellent (8×8) LEED pattern and a homogeneous layer with many grain boundaries and only occasional MP crystals, as shown in Fig. 12(b). The (8×8) structure always coexists with the (7×7) upon cooling below the (7×7)↔(1×1) transition temperature. A pure MP LEED pattern could only be obtained when the nitride layer was heated above 1350 K, due to the somewhat earlier and faster desorption of the (8×8) structure.

Nucleation and growth of the nitride layer not only depend upon temperature, NH_3 pressure and carbon contamination, but also upon the surface misorientation. This is clearly seen in the LEEM images of a Si(111) surface with the standard ±0.5° misorientation in Fig. 13. The (8×8) structure islands nucleate randomly at steps and develop rapidly a characteristic shape coupled with step bunching and terrace widening. The nitride growth front (towards the ten o'clock direction) has a sawtooth shape with the teeth pointing in the same $[\bar{1}\,\bar{1}2]$ direction as the apexes of triangles in earlier images. As growth proceeds the terraces widen considerably accompanied by step bunching, as evident by following the sequence of frames in Fig. 13. It should be noted that the (8×8) nitride layer shown in Fig. 13 was grown in the temperature range in which earlier studies by other workers obtained only the MP structure. This again demonstrates the decisive influence of contaminants or impurities on the formation of the MP structure. Terrace widening and step bunching were also observed on a Si(111) surface with an intentional 2.5° miscut towards $[11\bar{2}]$ in the STM. Comparing the clean vicinal surface in Fig. 14(a) with the same surface after nitridation in Fig. 14(b), it is obvious that the terraces have widened considerably, due to step bunching. In fact, the bunched steps have a facet-

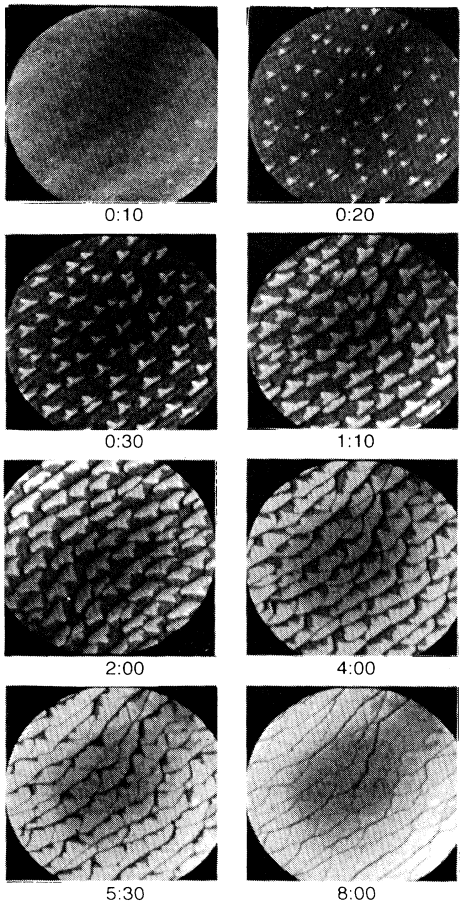

FIG. 13. LEEM growth sequence of (8×8) islands on a Si(111) surface with misorientation ±0.5°, exposed to 1×10^{-7} torr NH_3 at 1270 K, showing widening of terraces and step bunching as growth proceeds. Electron energy 3.6 eV. Field of view 10 μm.

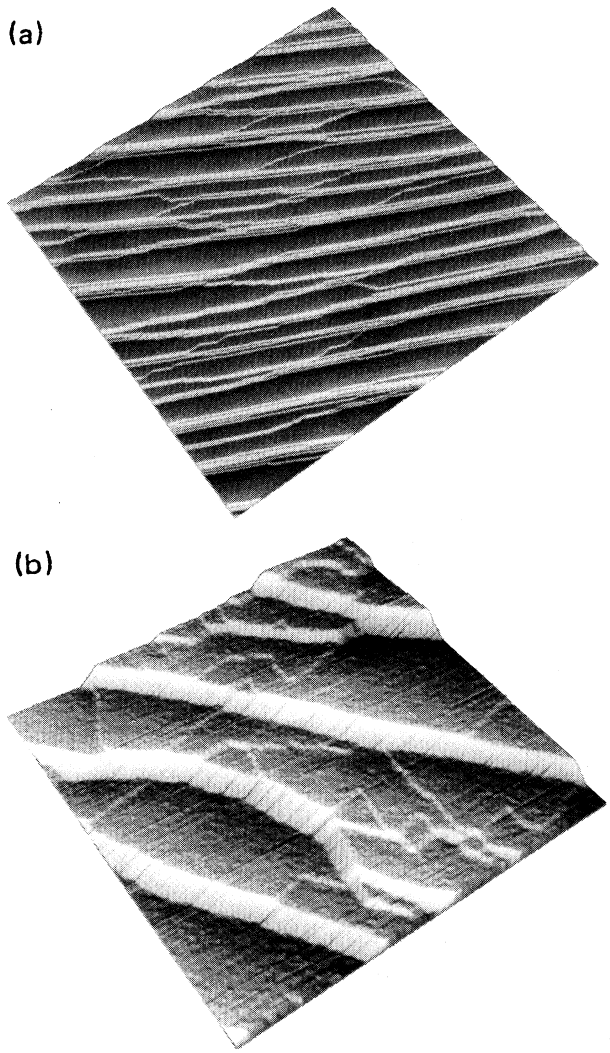

FIG. 14. 3D STM images of a Si(111) vicinal surface with 2.5° miscut towards $[11\bar{2}]$: (a) before, and (b) after exposure to 6×10^{-7} torr NH_3 for 3 min at 1220 K. Scan area is 200×200 nm^2 in both images. Sample bias is 2.0 V in (a) and 5.0 V in (b). Step-down direction is from top to bottom.

ed appearance. Our measurements show that these facets make an angle of $\sim 13°$ with the (111) surface, which make them (553) facets. Once again, as on the well-oriented surface in Figs. 7 and 8, triangular and hexagonal shapes of the (8×8) nitride layers appear on the terraces.

In view of the high desorption temperature and of the refractory nature of silicon nitride, one might expect that silicon nitride layers should be bound very strongly to the substrate and act as diffusion barriers for more weakly bound metals. We have checked this with deposition of Au, whose desorption temperature is lower than that of N from the Si(111) surface. Surprisingly, the nitride layer is completely displaced by Au far below the Si_2N desorption temperature with the appearance of LEED patterns and LEEM images characteristic for Au adsorption layers.[29] Thus, the desorption temperature is by no means a measure for the strength of bonding, which depends upon the specific chemical and electronic interactions in a more complex manner. Presumably the Au-Si interaction weakens the Si back bonds between the nitride layer and the substrate to such an extent that N can desorb as Si_2N at much lower temperatures than in the absence of Au.

IV. CONCLUSIONS

From the LEED patterns taken at low energies and the STM images, we have produced a structural model for the (8×8) nitride surface based on a $(\frac{8}{3}\times\frac{8}{3})$ overlayer on the Si(111)-(1×1) substrate, as shown in Figs. 3(a) and 3(b). The multiplet (MP) structure at higher temperatures consists of $(\frac{3}{4}\times\frac{3}{4})$ Si-N honeycombs azimuthally rotated, with respect to the Si(111) substrate by small angles depending on the splitting. In surface regions under prolonged electron beam irradiation, a singlet pattern was observed with additional $(3\sqrt{3}/4\times 3\sqrt{3}/4)$ spots. This unrotated structure has an additional N atom per unit mesh giving a composition of Si_3N_4.

The nucleation and growth of the (8×8) nitride layer bear many similarities to the (7×7) reconstruction of the clean Si(111) surface, as demonstrated by the STM and real-time LEEM images. The (8×8) islands nucleate predominantly on step edges and grow in a manner similar to the (7×7) domains, i.e., with the apex of the triangle pointing at the $[\bar{1}\,\bar{1}2]$ direction away from the step into the upper terrace. On misoriented Si(111) surfaces, growth of the nitride layer is accompanied by terrace widening and step bunching.

The MP structure, on the other hand, nucleates apparently randomly, at least on well-oriented surfaces, in the form of flat crystals. When surface contamination is visible, it nucleates only in contaminated regions and does so before (8×8) islands nucleate in clean regions. The MP structure has a much lower tendency to spread laterally than the (8×8) structure. In the present study, complete surface coverage with MP structure was not observed, even on the most contaminated surfaces.

ACKNOWLEDGMENT

This work was supported by the Office of Naval Research Grant No. N00014-94-1-0473. The acquisition of the LEEM was partly supported by the National Science Foundation grant DMR-9112021.

*Also at Physikalisches Institut, Technische Universität Clausthal, D-38678 Clausthal-Zellerfeld, Germany.

[1]V. I. Belyi, L. L. Vasilyeva, A. S. Ginovker, V. A. Gristsenko, S. M. Repinsky, S. P. Sinitsa, T. P. Smirnova, and F. L. Edelman, *Silicon Nitride in Electronics* (Elsevier, Amsterdam, 1988).

[2]J. T. Milek, *Silicon Nitride for Microelectronic Applications* (Plenum, New York, 1971).

[3]M. A. Hitchman and K. F. Jensen, *Chemical Vapor Deposition* (Academic, London, 1993).

[4]A. G. Schrott and S. F. Fain, Jr., Surf. Sci. **111**, 39 (1981); **123**, 204 (1982).

[5]K. Edamoto, S. Tanaka, M. Onchi, and M. Nishjima, Surf. Sci. **167**, 285 (1986).

[6]H.-C. Wang, R.-F. Lin, and X. Wang, Surf. Sci. **188**, 199 (1987).

[7]J. F. Delord, A. G. Schrott, and S. C. Fain, Jr., J. Vac. Sci. Technol. **17**, 517 (1980).

[8]C. Maillot, H. Roulet, and G. Dufour, J. Vac. Sci. Technol. B **2**, 316 (1984).

[9]A. J. van Bommel and F. Meyer, Surf. Sci. **8**, 381 (1967).

[10]R. Heckingbottom, in *The Structure and Chemistry of Solid Surfaces,* edited by G. A. Somorjai (Wiley, New York, 1969), p. 78-1.

[11]R. Heckingbottom and P. R. Wood, Surf. Sci. **36**, 594 (1973).

[12]M. Nishijima and K. Fujiwara, Solid State Commun. **24**, 101 (1977).

[13]T. Isu and K. Fujiwara, Solid State Commun. **42**, 477 (1982).

[14]S. Tanaka, M. Onchi, and M. Nishijima, Surf. Sci. **191**, L756 (1987).

[15]F. Boszo and Ph. Avouris, Phys. Rev. B **38**, 3937 (1988).

[16]B. G. Koehler, P. A. Coon, and S. M. George, J. Vac. Sci. Technol. B **7**, 1303 (1989).

[17]S. M. Cherif, J.-P. Lacharme, and C. A. Sebenne, Surf. Sci. **243**, 113 (1991); **274**, 257 (1992).

[18]E. A. Khramtsova, A. A. Saranin, and V. G. Lifshits, Surf. Sci. Lett. **280**, L259 (1993).

[19]W. D. Wiggins, R. J. Baird, and P. Wynblatt, J. Vac. Sci. Technol. **18**, 965 (1981).

[20]M. Nishijima, H. Kobayashi, K. Edamoto, and M. Onchi, Surf. Sci. **137**, 473 (1984).

[21]M. Nishijima, K. Edamoto, Y. Kubota, H. Kobayashi, and M. Onchi, Surf. Sci. **158**, 422 (1985).

[22]S. Yokumitsu, T. Anazawa, K. Ozawa, E. Miyazaki, K. Edamoto, and H. Kato, Surf. Sci. **317**, 143 (1994).

[23]Y. Bu, D. W. Shinn, and M. C. Lin, Surf. Sci. **276**, 184 (1992).

[24]J. C. S. Chu, Y. Bu, and M. C. Lin, Surf. Sci. **284**, 281 (1993).

[25]Ph. Avouris, F. Boszo, and R. J. Hamers, J. Vac. Sci. Technol. B **5**, 1387 (1987).

[26]Elmitec GmbHi.G., D-38678 Clausthal-Zellerfeld, Germany.

[27]E. Bauer, M. Mundschau, W. Swiech, and W. Telieps, J. Vac. Sci. Technol. A **9**, 1007 (1991).

[28]W. Telieps and E. Bauer, Surf. Sci. **162**, 163 (1985); Ber. Bunsenges Phys. Chem. **90**, 197 (1986).

[29]W. Swiech, E. Bauer, and M. Mundschau, Surf. Sci. **253**, 283 (1991).

[30]R. Wolkow and Ph. Avouris, Phys. Rev. Lett. **60**, 1049 (1988).
[31]Ph. Avouris, R. Wolkow, F. Bozso, and R. Hamers, in *SiO_2 and Its Interfaces,* edited by S. T. Pantelides and G. Lucovsky, MRS Symposia Proceedings No. 105 (Materials Research Society, Pittsburgh, 1988), p. 35.
[32]M. Mundschau, E. Bauer, W. Telieps, and W. Swiech, Philos. Mag. A **61**, 257 (1990).
[33]Y. Wei, L. Li, and I. S. T. Tsong, J. Vac. Sci. Technol. (to be published).

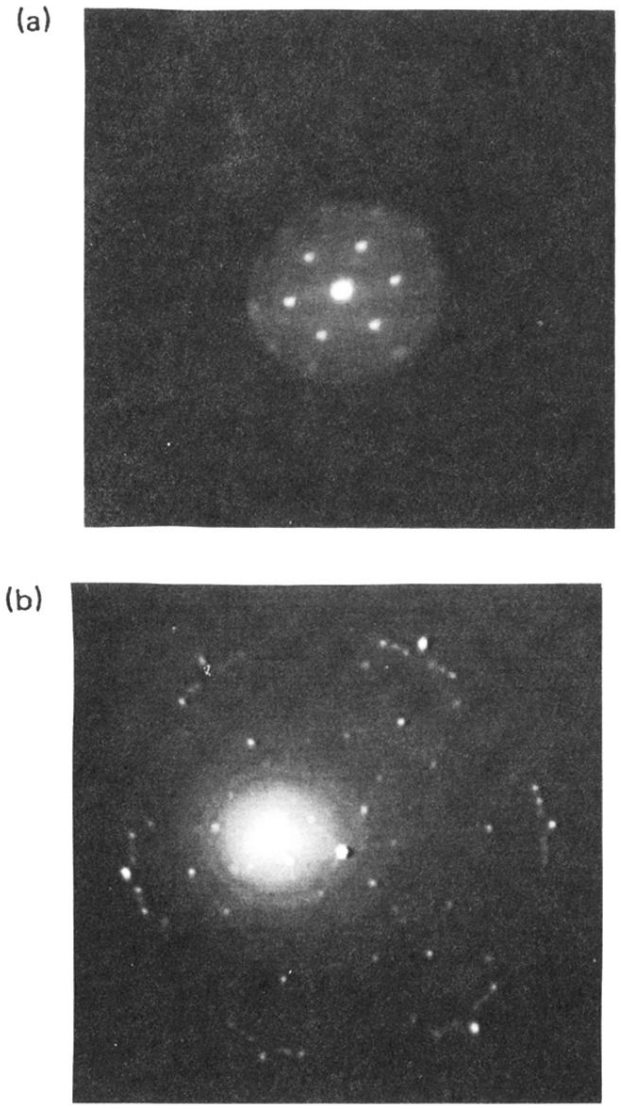

FIG. 1. LEED patterns of layers obtained by nitridation of Si(111) at 1140 K at 1×10^{-7} torr of NH_3 for 15 min: (a) Taken at 6.5 eV. Only the low-order beams of the (8×8) pattern appear. (b) Taken at 28 eV, showing the (8×8) plus sextet pattern. Higher-order beams, in particular the dominating $\frac{11}{8}$ order, are present.

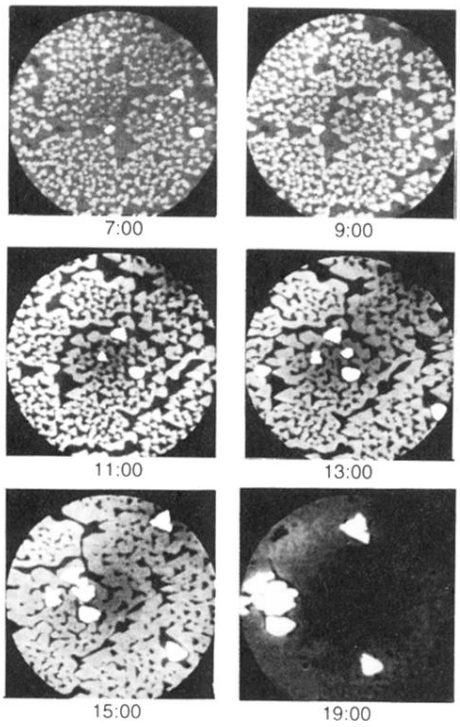

FIG. 10. LEEM images of later growth stages during exposure to 1×10^{-7} torr NH_3 at 1270 K. The brightest areas are $(\frac{3}{4}\times\frac{3}{4})$ multiplet structure islands. Electron energy 42 eV. Field of view 15 μm.

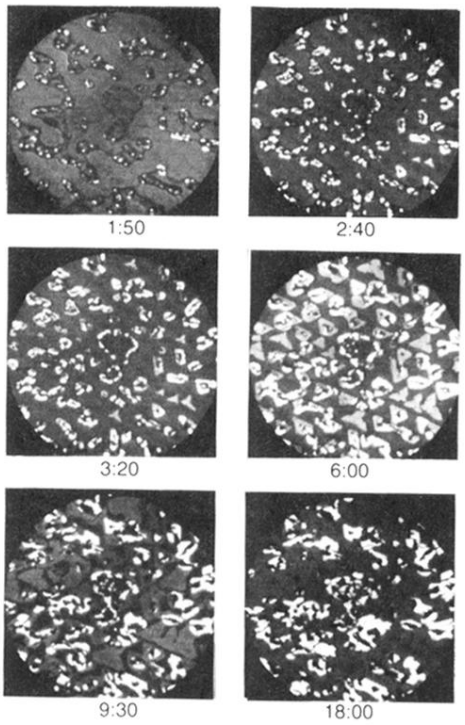

FIG. 11. LEEM growth sequence during exposure to 1.5×10^{-7} torr NH_3 at 1200 K, showing both $(\frac{3}{4}\times\frac{3}{4})$ islands (brightest) and (8×8) islands (less bright). Electron energy 42 eV. Field of view 15 μm.

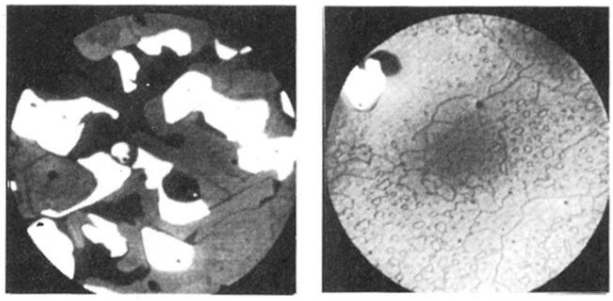

FIG. 12. LEEM images taken in the same growth sequence as in Fig. 10. (a) Area under prolonged electron irradiation after 25:00; and (b) area outside the irradiated region after 30:00. Brightest areas are $(\frac{3}{4}\times\frac{3}{4})$ islands. Electron energy 42 eV. Field of view 15 μm.

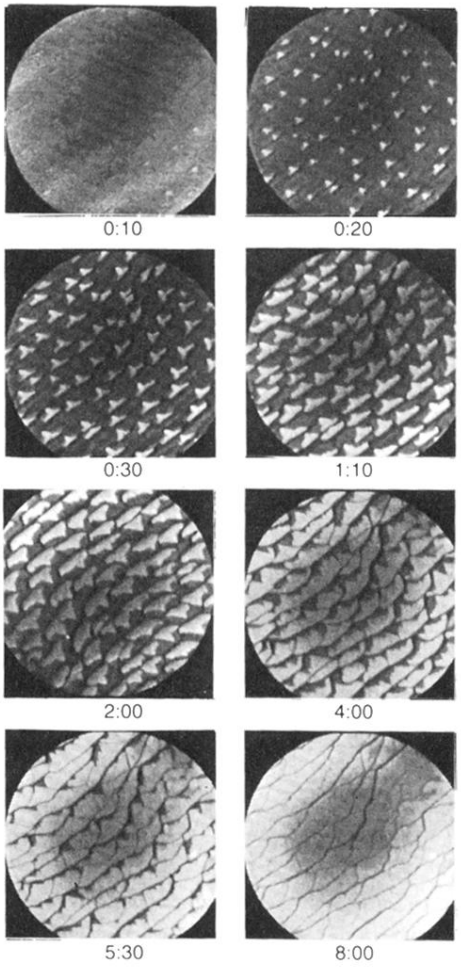

FIG. 13. LEEM growth sequence of (8×8) islands on a Si(111) surface with misorientation ±0.5°, exposed to 1×10^{-7} torr NH_3 at 1270 K, showing widening of terraces and step bunching as growth proceeds. Electron energy 3.6 eV. Field of view 10 μm.

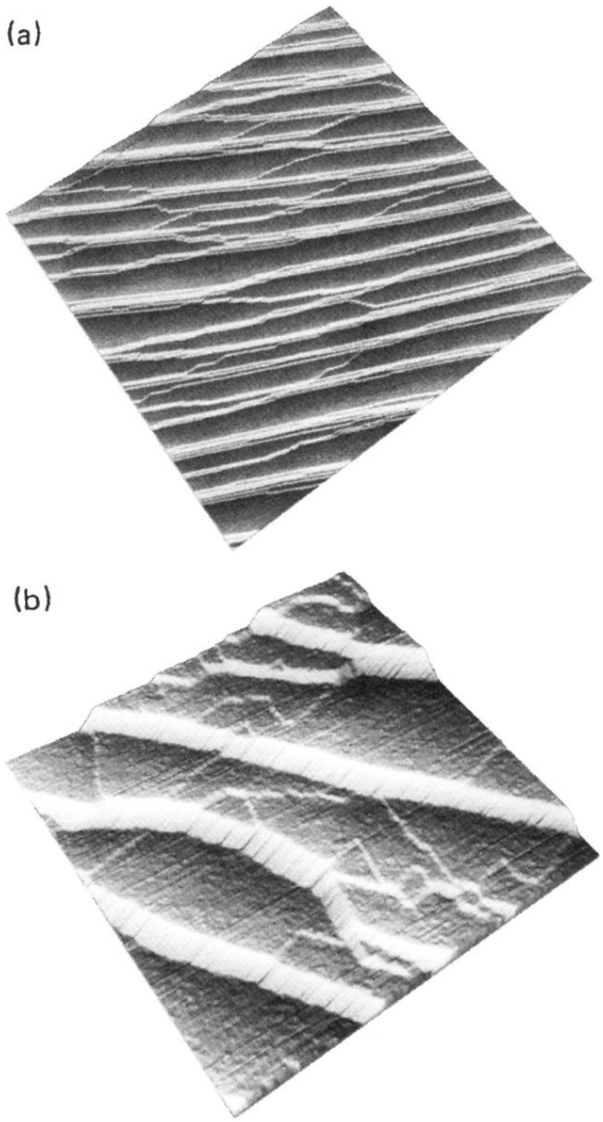

FIG. 14. 3D STM images of a Si(111) vicinal surface with 2.5° miscut towards $[11\bar{2}]$: (a) before, and (b) after exposure to 6×10^{-7} torr NH_3 for 3 min at 1220 K. Scan area is 200×200 nm^2 in both images. Sample bias is 2.0 V in (a) and 5.0 V in (b). Step-down direction is from top to bottom.

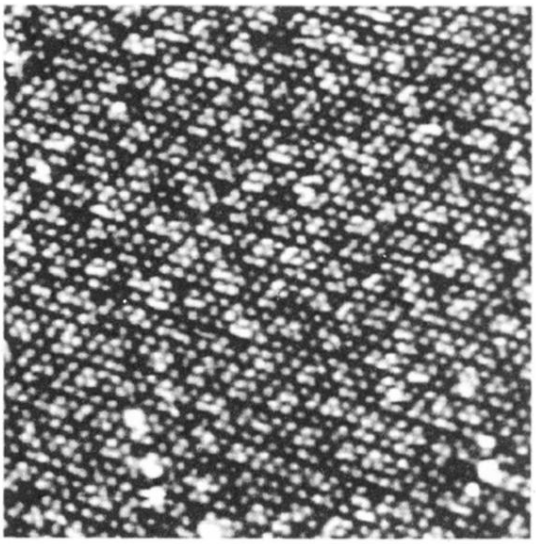

FIG. 2. A 365×365 Å^2 STM image of a nitride layer with $(\frac{8}{3} \times \frac{8}{3})$ structure. Nitridation of the Si(111) surface occurred at 1220 K at 6×10^{-7} torr of NH_3 for 15 min. Sample bias $= -4.0$ V.

(a)

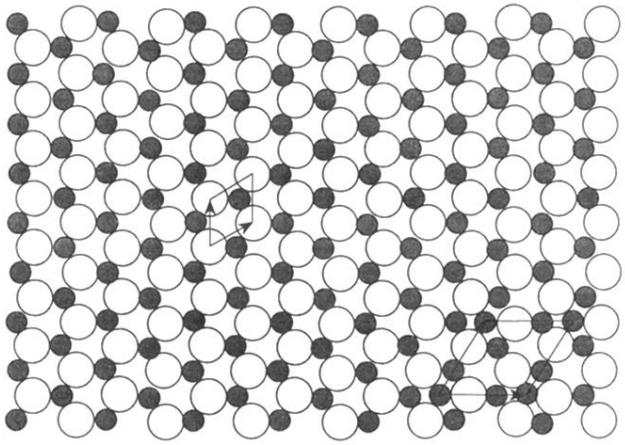

(b)

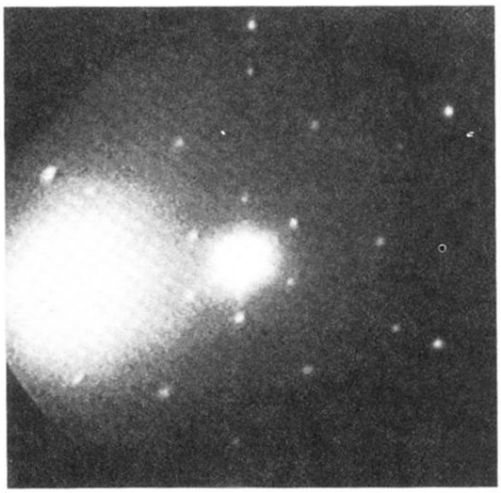

FIG. 4. (a) A model of the $(\frac{3}{4}\times\frac{3}{4})$ multiplet structure showing planar SiN honeycombs. The $(\frac{3}{4}\times\frac{3}{4})$ unit cell is shown near the center. The open circles represent Si and the shaded circles N. A $(3\sqrt{3}/4\times 3\sqrt{3}/4)$ unit cell is shown in the corner by adding extra N atoms in the center of the honeycombs to represent the singlet structure. (b) A singlet LEED pattern showing the extra $(3\sqrt{3}/4\times 3\sqrt{3}/4)$ spots. Taken at electron energy 33.6 eV.

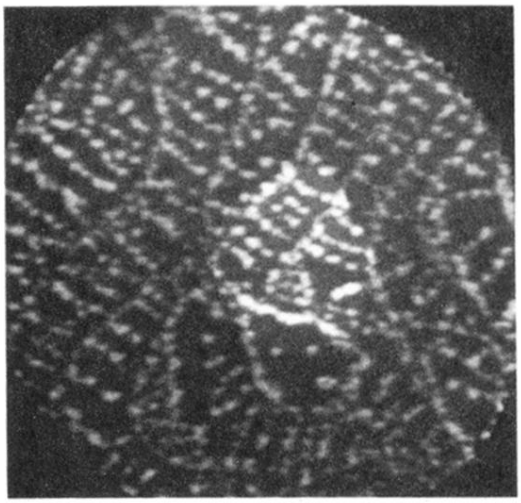

FIG. 5. LEEM image of the Si(111) surface saturated by exposure to 6×10^{-7} torr NH_3 for 15 min at room temperature and then annealed to 1210 K. Taken with $\frac{3}{8}$ order beam. Electron energy 2.7 eV. Field of view 6 μm.

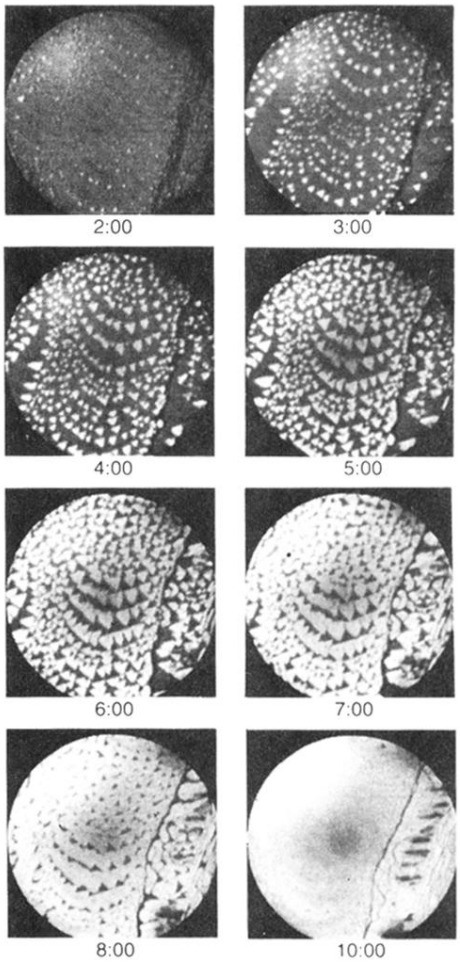

FIG. 6. LEEM video images of growth sequence of (8×8) nitride islands, during exposure to 2×10^{-7} torr NH_3 at 1260 K. Elapsed time in minutes is indicated below each frame, with 0:00 being the time when NH_3 was admitted into the LEEM sample chamber. The (8×8) areas are bright and (1×1) areas dark. The line running north-south on the right-hand side of the images is a scratch on the surface. Electron energy 42 eV. Field of view 10 μm.

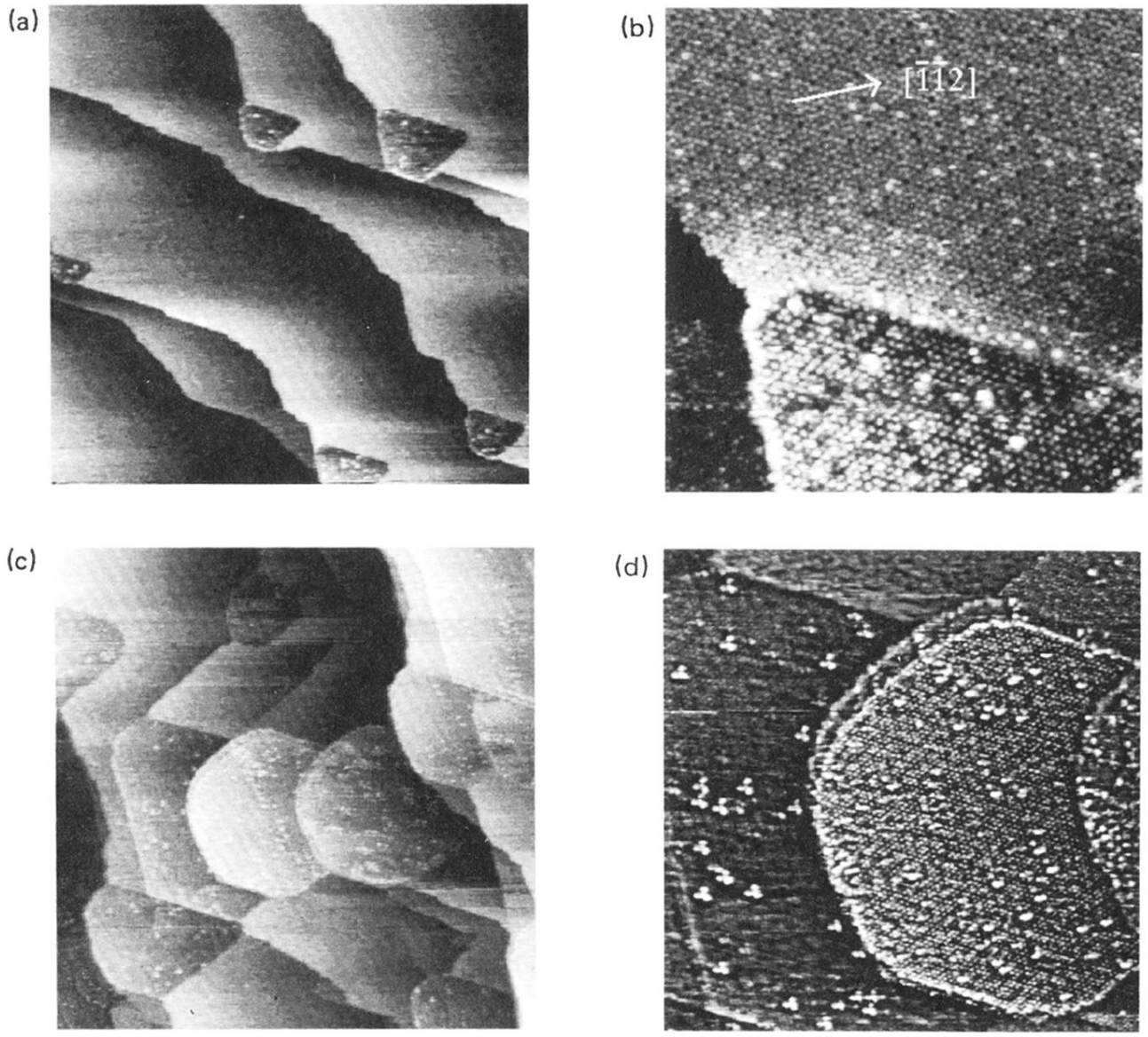

FIG. 7. STM images of initial stages of nitridation. The well-oriented Si(111) surface was exposed to 2×10^{-7} torr NH_3 for 10 sec at 1220 K (a) and (b) and subsequently annealed at 1320 K (c) and (d). Scan areas: (a) 250×250 nm^2, (b) 514×514 Å^2, (c) 250×250 nm^2, and (d) 850×850 Å^2. Sample bias: (a) and (b) -3.5 V; (c) and (d) 4.0 V. The triangular (8×8) structure is 2.1 Å higher than the lower (7×7) terrace and 1.0 Å below the (7×7) structure on the same terrace in image (b).

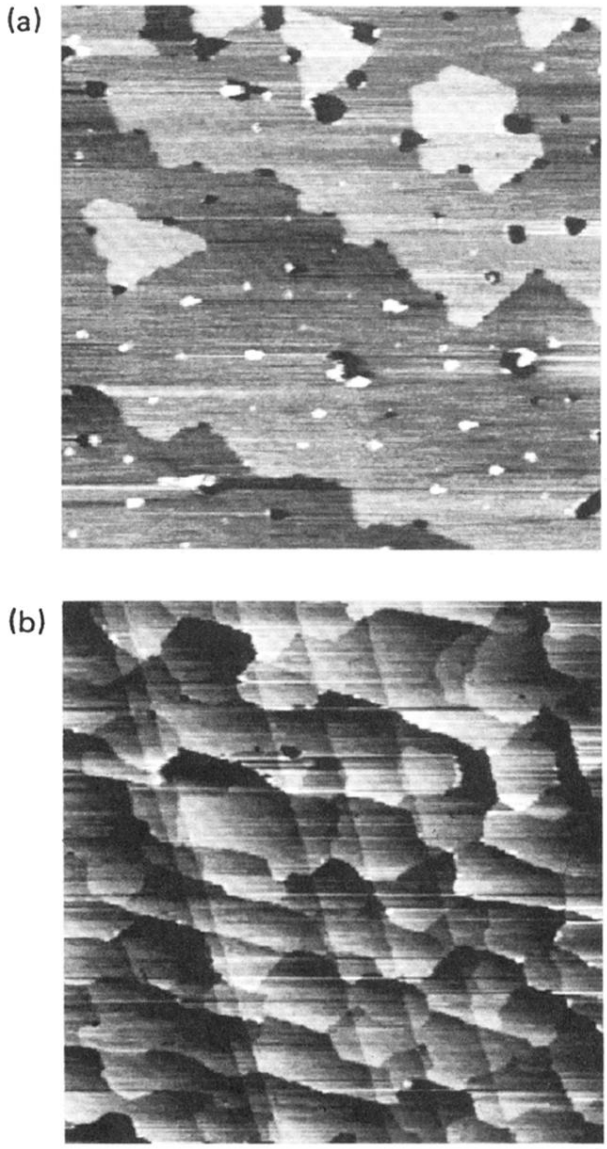

FIG. 8. STM images of a well-oriented Si(111) surface; (a) after exposure to 6×10^{-7} torr NH_3 for 15 min at 1220 K; and (b) subsequently annealed at 1320 K. Scan area is 1×1 μm^2 in both images. Sample bias is 5.0 V.

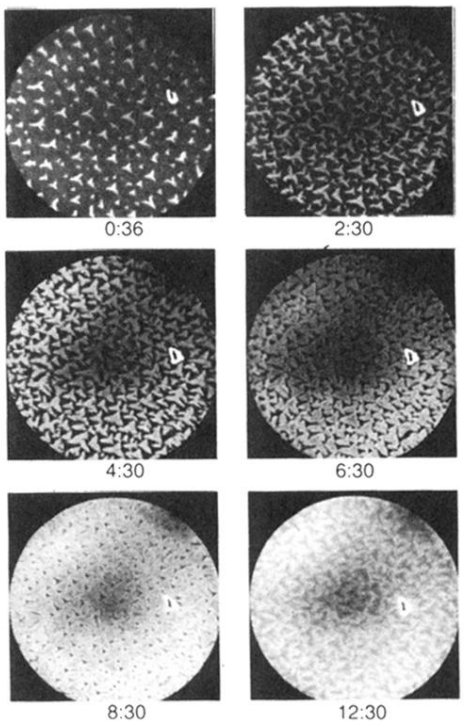

FIG. 9. LEEM video images of growth sequence of dendritic (8×8) nitride islands during exposure to 2×10^{-7} torr NH_3 at 1180 K. Elapsed time in minutes is indicated below each frame. Electron energy 45.4 eV. Field of view 15 μm.